

LETTER

Open Access



Sweat-permeable electronic skin with a pattern of eyes for body temperature monitoring

Jeong Hyeon Kim^{1,2}, Daniel J. Joe³ and Han Eol Lee^{1,2*} 

Abstract

Human-machine interface has been considered as a prominent technology for numerous smart applications due to their direct communication between humans and machines. In particular, wearable electronic skins with a free form factor have received a lot of attention due to their excellent adherence to rough and wrinkled surfaces such as human skin and internal organs. However, most of the e-skins reported to date have some disadvantages in terms of mechanical instability and accumulation of by-products at the interface between the human skin and the device. Here, we report a mechanically stable e-skin via a newly designed pattern named the “eyes.” The ingeniously designed pattern of the eyes allowed mechanical stress and strain to be dissipated more effectively than other previously reported patterns. E-skin permeability of by-product was experimentally confirmed through sweat removal tests, showing superior sweat permeability compared to conventional e-skins. Finally, the real-time monitoring of the body temperature was carried out using our resistive-type thermometer in the e-skin.

Keywords Sweat permeability, Electronic skin, Body temperature monitoring sensor

Introduction

With the beginning of advanced information age, Internet of Things (IoT) technologies have received much attention in recent decades, including human-machine interface (HMI), artificial intelligence (AI), and machine learning (ML) as a tool for info-communication between objects. These IoT techniques have been intensively investigated by many researchers due to their easy accessibility, rapid data processing and wide applicability

[1–6]. In particular, HMI technology has been highlighted for use in numerous smart applications (e.g. voice recording, touch panels, and wearable electronic devices, etc.) thanks to its direct connectivity between man and machine [7–12].

Among various types of HMI devices, wearable electronic skins (e-skins) have been considered as an emerging platform for personal electronics with their free form factor, which can be attached to uneven and corrugated surfaces such as human skin and internal organs [13–18]. Although the previously reported work has demonstrated health monitoring sensors in e-skins (e.g., electrocardiogram (ECG) electrodes, photoplethysmogram (PPG) devices, and heart rate sensors), they still have some issues including mechanical instability and by-product accumulation at the interface between the human skin and the device [19–21]. In detail, the e-skin attached to the skin becomes constantly stressed by the bending and stretching through body movements in daily life, leading to device degradation and inaccurate sensing properties

*Correspondence:

Han Eol Lee
haneol@jbnu.ac.kr

¹ Division of Advanced Materials Engineering, Jeonbuk National University, 567 Baekje-daero, Deokjin-gu, Jeonju-si, Jeollabuk-do 54896, Republic of Korea

² Department of JBNU-KIST Industry-Academia Convergence Research, Jeonbuk National University, 567 Baekje-daero, Deokjin-gu, Jeonju-si, Jeollabuk-do 54896, Republic of Korea

³ Safety Measurement Institute, Korea Research Institute of Standards and Science (KRISS), 267 Gajeong-ro, Yuseong-gu, Daejeon 34113, Republic of Korea



© The Author(s) 2023. **Open Access** This article is licensed under a Creative Commons Attribution 4.0 International License, which permits use, sharing, adaptation, distribution and reproduction in any medium or format, as long as you give appropriate credit to the original author(s) and the source, provide a link to the Creative Commons licence, and indicate if changes were made. The images or other third party material in this article are included in the article's Creative Commons licence, unless indicated otherwise in a credit line to the material. If material is not included in the article's Creative Commons licence and your intended use is not permitted by statutory regulation or exceeds the permitted use, you will need to obtain permission directly from the copyright holder. To view a copy of this licence, visit <http://creativecommons.org/licenses/by/4.0/>.

[22–25]. In addition, human by-products from the skin surface affect the attached e-skin, resulting in unwanted device delamination and skin troubles [26–28]. These problems need to be solved to sustain the lives of vulnerable people who require continuous monitoring of their vital signs. For example, patients with heat allergies suffer life-threatening symptoms (e.g. heat stroke, heat cramps, heat syncope) from sudden increases in body temperature during daily activities [29–31]. The elderly, infirm and infants also require constant physiological monitoring due to their lack of control over their body temperature [32–34].

Herein, we introduce a perforated e-skin with an eyes-patterned structure to monitor body temperature in real time. The eyes-pattern in the e-skin was theoretically modelled using finite element analysis (FEA) simulation to enhance mechanical properties and sweat permeability compared to other structures, such as auxetic kirigami and circular hole patterns. The resistive-type temperature sensor was fabricated at the center of a 10 μm-thick polyimide (PI) thin film to minimize stress localization. The developed e-skin maintained its mechanical and electrical performance under bending conditions with a

radius of curvature of 500 μm. The sweat permeability of the developed device was analyzed by verifying the color change of litmus paper on the e-skin attached to the skin. Finally, we monitored the body temperature in real time using the resistive-type body temperature monitoring (BTM) patch, showing the coincidence of tendency with the conventional thermometer.

Result and discussion

Figure 1a shows the fabrication process and a three-dimensional schematic of the eyes-patterned e-skin. The detailed process is as follows: (i) 200 nm-thick aluminum (Al) and 5 μm-thick polyimide (PI) thin films were sequentially deposited on a rigid p-type Si substrate. (ii) Cr and Au thin films (thickness of 50 and 300 nm, respectively) were deposited and patterned by conventional complementary metal-oxide-semiconductor (CMOS) process to fabricate electrode and resistive temperature sensor. After covering the metal thin films with the PI passivation layer, a 200 nm-thick Cu etching mask with the desired patterns such as circular holes, kirigami, or eyes-patterns was fabricated on the PI surface, and then the whole layers were patterned by inductively coupled

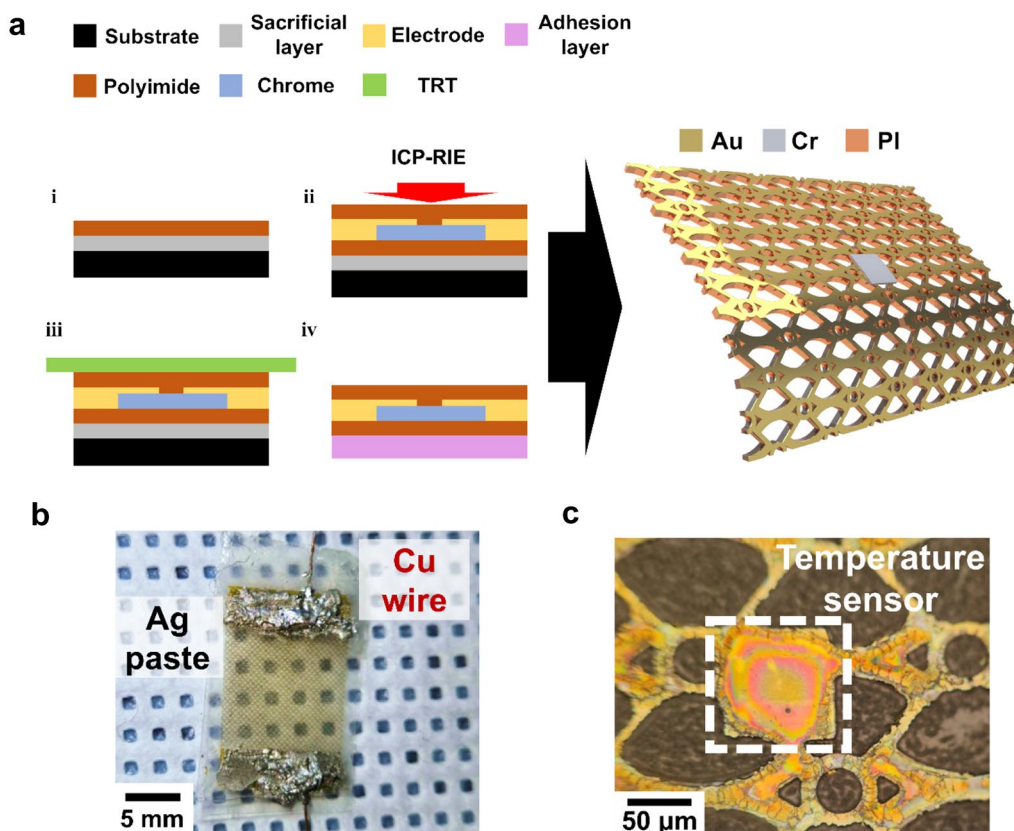


Fig. 1 a Fabrication process of eyes-patterned e-skin with BTM sensor. b Optical image of the wearable BTM sensor. c Magnified microscopic image of the temperature sensor in the developed e-skin

plasma-reactive ion etching (ICP-RIE) to provide the permeability for the e-skin. (iii) The ultrathin 10 μm-thick device was attached to a temporary substrate (thermal release tape; TRT), and the device was peeled off from the mother Si substrate through an electrochemical lift-off (ECL) process. The Al sacrificial layer on the mother wafer was removed by electrochemical reaction in 0.9 wt% NaCl solution at 3 V bias. (iv) After transferring the device to the TRT substrate, a polydimethylsiloxane (PDMS) adhesive layer was coated onto the back side of the e-skin. Finally, the temporary substrate was delaminated at 120 °C (See the [Experiments](#) section for a detailed description of the e-skin fabrication process). Figure 1b is an optical image of the fabricated eyes-patterned e-skin with body temperature monitoring (BTM) sensor electrically interconnected with Cu wires through Ag paste. The Cr-based resistive temperature sensor was successfully fabricated on the eyes-patterned e-skin as shown in Fig. 1c.

Because the skin-attached e-skin is constantly stressed by bending and stretching motions during daily activities, the e-skin need to provide mechanical stability to prevent the device from breaking or malfunctioning [35–38]. A novel eyes-pattern was developed to prevent the aforementioned issues in advance. Prior to the experiment, the mechanical stability of the eyes-pattern was theoretically analyzed by FEA simulation to compare with that of other patterns. To calculate the localized stresses and strains of the designed patterns in the e-skin, FEA calculations were performed using Ansys Workbench. Three typical geometric (TG) models, eyes, circular holes, and auxetic kirigami patterns were designed with the same

scale in hole diameter, line width, and pattern distribution. The static structure calculation sequence was used to evaluate the von Mises stress using Eq. 1 below:

$$\sigma_{vm} = \sqrt{\frac{(\sigma_1 - \sigma_2)^2 + (\sigma_2 - \sigma_3)^2 + (\sigma_3 - \sigma_1)^2}{2}} \tag{1}$$

where σ_1 , σ_2 , and σ_3 are the stress components of each axis in three dimensions. The 45 μm displacement was applied to both ends of each geometry to observe the changes in localized stress and strain. The linear elastic property was used for the PI material (material density: 1.42 g/cm³, Young’s modulus: 2.5 GPa, and Poisson’s ratio: 0.34).

Figure 2a depicts the calculated stress distribution images of the e-skins with various patterns. Less than 30% of the applied strain conditions, all patterns in the 300×300 μm² scale (minimum line width: 12 μm, hole diameter: 75 μm) showed stress localization at the edge of the structure. However, as shown in Fig. 2b-i, the eyes-pattern exhibited a maximum localized stress of about 943.3 MPa, which was 48.7% and 60.8% lower than the auxetic kirigami (about 1839.9 MPa) and circular hole patterns (about 2408.8 MPa), respectively. Figure 2b-ii displays the localized strain of the patterns, showing that the eyes-pattern has the lowest localized strain of 43.11% compared to that of other structures (auxetic kirigami: 74.53%, circular hole: 101.41%), shown in Additional file 1: Table S1. These results indicate that the newly designed eyes-pattern has superior mechanical properties for stress relief and prevention of crack initiation

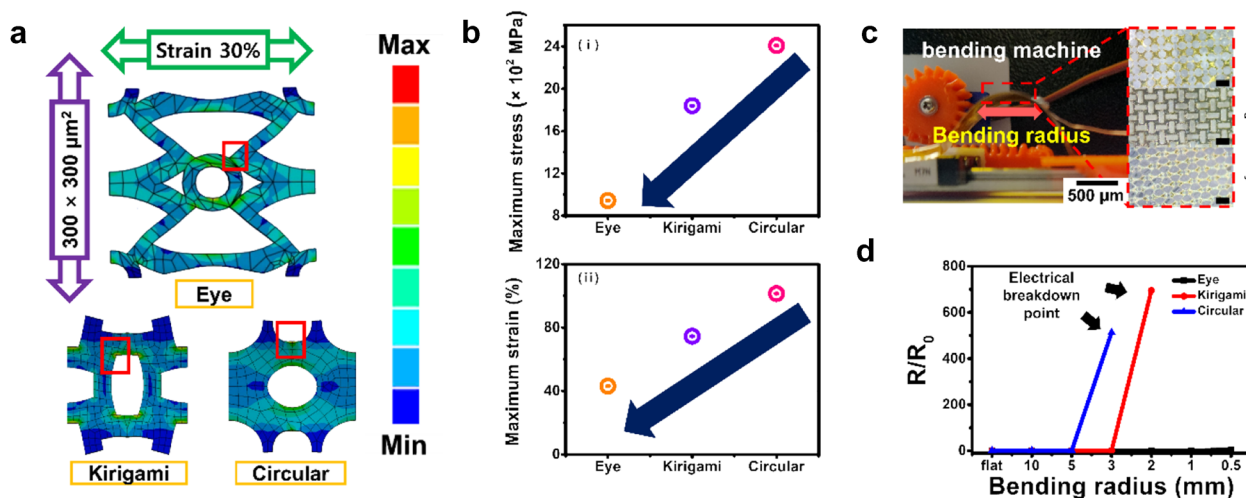


Fig. 2 a Simulated stress mapping images of various e-skin structures. b (i) Comparison graph of the calculated maximum stress and (ii) strain in three different e-skins. c Optical images of the bending test (left) and various e-skin structures (right, scale bar: 500 μm). d Bending test results for each of the e-skin structures

and propagation compared to normal PI film (maximum strain: < 20%) [39]. In order to experimentally confirm the mechanical stability of the patterns, the bending test was performed with various radii of curvature using an Arduino-based bending machine, as shown in Fig. 2c. Figure 2d depicts that the resistance changes of the eyes-patterned electrode were negligible due to the efficient stress dissipation along the entire structure, whereas the auxetic kirigami and circular hole-patterned e-skins were broken at the bending condition of 3 and 5 mm, respectively. Since the minimum bending radius of the human body is known to be about 3.8 mm [40, 41], it is noteworthy that the eyes-patterned e-skin can be considered as an optimal structure for excellent stress-resistant wearable e-skin during body movements.

In order to build practical wearable devices for real-time monitoring of vital signs, the accuracy of the sensing device without malfunctioning due to accumulation of skin by-products at the skin/e-skin interface is critical. As shown in Fig. 3a, our eyes-pattern in the e-skin has the periodic and porous structure with auxetic kirigami pattern, which was predicted to efficiently remove by-products at the skin-device interface due to similar size and distribution with human sweat pores [27]. To experimentally verify the by-product permeability of our e-skin, penetration tests of sweat, one of the representative skin by-products, were conducted through the eyes-patterned e-skin and a conventional e-skin for an hour. The amount of sweat penetration was determined by comparing the color changes of the litmus paper between our e-skin and

the conventional e-skin. Figure 3b displays the experimental setup for the sweat penetration tests. The litmus papers on the conventional e-skin and our e-skin were attached to a 3×3 mm²-sized hole in the nitrile glove, which was used to accelerate the perspiration of the hand. Figure 3c shows the time-lapse images of the color changes of litmus papers attached to our e-skin and the conventional e-skin. Although the litmus paper on the conventional e-skin exhibited no color change, the litmus paper on our e-skin was wetted by excessive perspiration, showing color changes from yellow (pH 7) to green (pH 8). This result was attributed that our e-skin prevented sweat accumulation [42]. The area of color change was quantified using ImageJ, an image analysis tool. During a one hour-long perspiration test, the area percentage of color change in the litmus paper on our e-skin changed to 45.04%, which was remarkable compared to that on the conventional e-skin (Additional file 1: Fig. S1). These results demonstrate that our e-skin has notable sweat permeability and is suitable for daily activation without accumulation of skin by-products.

Finally, our e-skin with excellent mechanical stability and sweat permeability was applied to real-time body temperature monitoring via a resistive-type BTM sensor. The reliability of our BTM sensor was verified by comparison with a conventional infrared (IR) thermometer (Fig. 4a). As the temperature increased from 20 °C to 90 °C, the BTM sensor showed a linear increase in resistance from 204 Ω to 682 Ω, showing the same trend as a conventional IR thermometer (average resistance

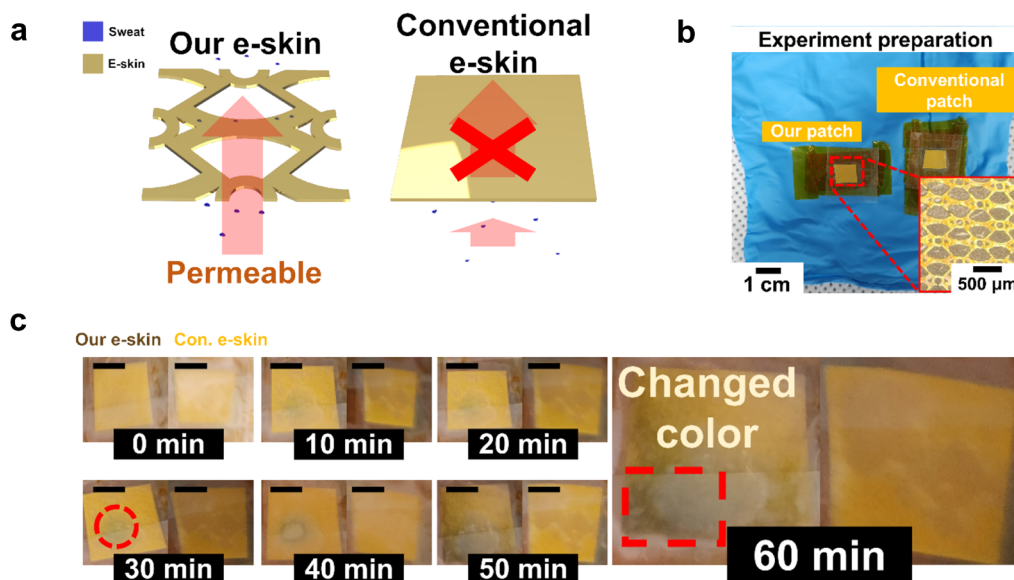


Fig. 3 a Sweat-permeability of eyes-patterned e-skin compared to conventional e-skin. b Optical image of the sweat-permeability test of the e-skins. The inset image shows a magnified microscopic image of the eyes-structured e-skin. c Color-changed images of litmus paper to monitor sweat permeability of e-skins (scale bar: 500 μm)

Experiments

Fabrication of the patterned e-skin

The Al sacrificial layer was deposited on a 4-inch Si substrate by thermal evaporation (VEV-503, VTS Corporation). Next, polyimide solution (PI, Sigma-Aldrich) was spin-coated onto the Si surface at 3000 rpm and baked sequentially at 110 °C (3 min), 130 °C (3 min), and 250 °C (1 h) to cure the film by evaporating the solvent. An Au electrode layer (300 nm) was deposited on the bottom PI by e-beam evaporation and patterned by conventional CMOS processes. A resistive metal layer (Cr, 20 nm) of $100 \times 100 \mu\text{m}^2$ was formed by interconnecting the Au electrodes to fabricate the BTM sensor. After coating the top PI layer, e-beam evaporation was used to create a Cu mask layer (200 nm). The ICP-RIE process was carried out under optimized conditions (50 sccm O₂ flow, 20 mTorr working pressure, 300 W ICP and 150 W bias). After the ECL process, the PDMS adhesion layer was applied to the backside of the delaminated e-skin and then cured at 70 °C for one hour.

Evaluation of mechanical properties

The Cu-wire was electrically connected to the metal pads of the e-skin with silver epoxy (MG Chemicals, 8331 S). To verify electrical performance under various bending radii from flat to 0.5 mm, a conventional linear stage motor (LSM-NK235603, Motorbank) and source meter (Keithley 2450, Tektronix) were used at 1 V bias. The bending curvature radius was accurately controlled from flat to 0.5 mm through the programmed codes in the bending motion system.

Evaluation of the BTM performance

The resistive-type BTM sensor was integrated into the e-skin. The BTM sensor attached to the forearm measured the change in resistance of the sensor during exercise and reset in real time. For continuous perspiration, we fulfilled the push-up 30 times at each cycle and had 5 min resting time.

Supplementary Information

The online version contains supplementary material available at <https://doi.org/10.1186/s40486-023-00170-1>.

Additional file 1: Figure S1. Photographs of color-changed litmus papers and images of tool analysis results. **Table S1.** FEA simulation results of the designed pattern and other patterns.

Acknowledgements

Not applicable.

Author contributions

Experiment design and conceptualization: JK and HL. Methodology and data analysis: JK and HL. Supervision: HL. Writing and editing of the manuscript: JK, DJ, and HL. All authors read and approved the final manuscript.

Funding

This research in JBNU was supported by National University Development Project at Jeonbuk National University in 2022. This work in KRIS was supported by Development of Measurement Standards and Technology for Biomaterials and Medical Convergence funded by Korea Research Institute of Standards and Science (KRIS—2022—GP2022-0006) and the National Research Foundation of Korea (NRF) grants funded by the Ministry of Science, ICT and Future Planning (MSIT) (NRF-2022R1A4A3033320 and Nano-Material Technology Development Program 2009–0082580).

Availability of data and materials

All data in this study is included in this published article.

Declarations

Ethics approval and consent to participate

Not applicable.

Consent for publication

Authors consent the SpringerOpen license agreement to publish the article.

Competing interests

The authors declare that they have no competing interests.

Received: 26 July 2023 Accepted: 3 August 2023

Published online: 15 September 2023

References

1. Barcelo M, Correa A, Llorca J, Tulino AM, Vicario JL, Morell A (2016) IoT-cloud service optimization in next generation smart environments. *IEEE J Sel Areas Commun* 34(12):4077–4090
2. Marjani M, Nasaruddin F, Gani A, Karim A, Hashem IAT, Siddiqua A, Yaqoob I (2017) Big IoT data analytics: architecture, opportunities, and open research challenges. *IEEE Access* 5:5247–5261
3. Lee K, Chae HY, Park K, Lee Y, Cho S, Ko H, Kim JJ (2019) A multi-functional physiological hybrid-sensing e-skin integrated interface for wearable IoT applications. *IEEE Trans Biomed Circuits Syst* 13(6):1535–1544
4. Kim MH, Cho CH, Kim JS, Nam TU, Kim WS, Lee TI, Oh JY (2021) Thermo-electric energy harvesting electronic skin (e-skin) Patch with reconfigurable carbon nanotube clays. *Nano Energy* 87:106156
5. Li D, Zhou J, Yao K, Liu S, He J, Su J, Qu Q, Gao Y, Song Z, Yiu C, Sha C, Sun Z, Zhang B, Li J, Huang L, Xu C, Wong TH, Huang X, Li J, Ye R, Wei L, Zhang Z, Guo X, Dai Y, Xie Z, Yu X (2022) Touch IoT enabled by wireless self-sensing and haptic-reproducing electronic skin. *Sci Adv* 8(51):eade2450
6. Niu H, Li H, Gao S, Li Y, Wei X, Chen Y, Yue W, Zhou W, Shen G (2022) Perception-to-cognition tactile sensing based on artificial-intelligence-motivated human full-skin bionic electronic skin. *Adv Mater* 34(31):2202622
7. Lee JH, Ahn Y, Lee HE, Jang YN, Park AY, Kim S, Jung YH, Sung SH, Shin JH, Lee SH, Park SH, Kim KS, Jang MS, Kim BJ, Oh SH, Lee KJ (2023) Wearable surface-lighting micro-light-emitting diode patch for melanogenesis inhibition. *Adv Healthc Mater* 12(1):2201796
8. Kang SM, Lee HE, Wang HS, Shin JH, Jo W, Lee Y, Lee H, Lee D, Kim YH, Kim TS, Lee KJ, Bae BS (2021) Self-powered flexible full-color display via dielectric-tuned hybrimer triboelectric nanogenerators. *ACS Energy Lett* 6(11):4097–4107
9. Lee HE (2021) Novel bio-optoelectronics enabled by flexible micro light-emitting diodes. *Electronics* 10(21):2644
10. Ding W, Wang AC, Wu C, Guo H, Wang ZL (2019) Human-machine interfacing enabled by triboelectric nanogenerators and tribotronics. *Adv Mater Technol* 4(1):1–16
11. Park S, Shin BG, Jang S, Chung K (2020) Three-dimensional self-healable touch sensing artificial skin device. *ACS Appl Mater Interfaces* 12(3):3953–3960
12. Zeng X, Liu Y, Liu F, Wang W, Liu X, Wei X, Hu Y (2022) A bioinspired three-dimensional integrated e-skin for multiple mechanical stimuli recognition. *Nano Energy* 92:106777

13. Wang L, Jiang K, Shen G (2021) Wearable, implantable, and interventional medical devices based on smart electronic skins. *Adv Mater Technol* 6(6):1–18
14. Norton JJS, Lee DS, Lee JW, Lee W, Kwon O, Won P, Jung SY, Cheng H, Jeong JW, Akce A, Umunna S, Na I, Kwon YH, Wang XQ, Liu Z, Paik U, Huang Y, Bretl T, Yeo WH, Rogers JA (2015) Soft curved electrode systems capable of integration on the auricle as a persistent brain-computer interface. *Proc Natl Acad Sci* 112(13):3920–25
15. Tian L, Zimmerman B, Akhtar A, Yu K, Moore M, Wu J, Larsen R, Lee J, Li J, Liu Y, Metzger B, Qu S, Guo X, Mathewson K, Fan J, Cornman J, Fatina M, Xie Z, Ma Y, Rogers J (2019) Large-area MRI-compatible epidermal electronic interfaces for prosthetic control and cognitive monitoring. *Nat Biomed Eng* 3(3):194–205
16. Cho KW, Sunwoo SH, Hong YJ, Koo JH, Kim JH, Baik S, Hyeon T, Kim DH (2022) Soft bioelectronics based on nanomaterials. *Chem Rev* 122(5):5068–5143
17. Jo M, Min K, Roy B, Kim S, Lee S, Park JY, Kim S (2018) Protein-based electronic skin akin to biological tissues. *ACS Nano* 12(6):5637–5645
18. Park YJ, Sharma BK, Shinde SM, Kim MS, Jang B, Kim JH, Ahn JH (2019) All MoS₂-based large area, skin-attachable active-matrix tactile sensor. *ACS Nano* 13(3):3023–3030
19. Li WD, Ke K, Jia J, Pu JH, Zhao X, Bao RY, Liu ZY, Bai L, Zhang K, Yang MB (2022) Recent advances in multiresponsive flexible sensors towards e-skin: a delicate design for versatile sensing. *Small* 18(7):2103734
20. Lee H, Lee W, Lee H, Kim S, Alban MV, Song J, Kim T, Lee S, Yoo S (2021) Organic-inorganic hybrid approach to pulse oximetry sensors with reliability and low power consumption. *ACS Photonics* 8(12):3564–3572
21. Cai YW, Zhang XN, Wang GG, Li GZ, Zhao DQ, Sun N, Li F, Zhang HY, Han JC, Yang Y (2021) A flexible ultra-sensitive triboelectric tactile sensor of wrinkled PDMS/MXene composite films for E-skin. *Nano Energy* 81:105663
22. Lee HE, Lee D, Lee TI, Jang J, Jang J, Lim YW, Shin JH, Kang SM, Choi GM, Joe DJ, Kim JH, Lee SH, Park SH, Park CB, Kim TS, Lee KJ, Bae BS (2022) Siloxane hybrid material-encapsulated highly robust flexible LEDs for biocompatible lighting applications. *ACS Appl Mater Interfaces* 14(24):28258–28269
23. Lee HE, Shin JH, Lee SH, Lee JH, Park SH, Lee KJ (2019) Flexible micro light-emitting diodes for wearable applications. *Proc SPIE* 10940:52
24. Yang X, Zhang M, Gong S, Sun M, Xie M, Niu P, Pang W (2023) Chest-laminated and sweat-permeable e-skin for speech and motion artifact-insensitive cough detection. *Adv Mater Technol* 8(4):1–12
25. Peng X, Dong K, Zhang Y, Wang L, Wei C, Lv T, Wang ZL, Wu Z (2022) Sweat-permeable, biodegradable, transparent and self-powered chitosan-based electronic skin with ultrathin elastic gold nanofibers. *Adv Funct Mater* 32(20):2112241
26. Webb RC, Bonifas AP, Behnaz A, Zhang Y, Yu KJ, Cheng H, Shi M, Bian Z, Liu Z, Kim YS, Yeo WH, Park JS, Song J, Li Y, Huang Y, Gorbach AM, Rogers JA (2013) Ultrathin conformal devices for precise and continuous thermal characterization of human skin. *Nat Mater* 12(10):938–944
27. Yeon H, Lee H, Kim Y, Lee D, Lee Y, Lee JS, Shin J, Choi C, Kang JH, Suh JM, Kim H, Kum HS, Lee J, Kim D, Ko K, Ma BS, Lin P, Han S, Kim S, Kim J (2021) Long-term reliable physical health monitoring by sweat pore-inspired perforated electronic skins. *Sci Adv* 7(27):eabg8459
28. Leung DYM, Calatroni A, Zaramela LS, LeBeau PK, Dyjack N, Brar K, David G, Johnson K, Leung S, Gama MR, Liang B, Rios C, Montgomery MT, Richers B N, Hall CF, Norquest KA, Jung J, Bronova I, Kreimer S, Talbot CC, Crumrine D, Cole RN, Elias P, Zengler K, Seibold MA, Berdyshev E, Goleva E (2019) The nonlesional skin surface distinguishes atopic dermatitis with food allergy as a unique endotype. *Sci Transl Med* 11(480):1–13
29. Abajian M, Schoepke N, Altrichter S, Zuberbier HCT, Maurer M (2014) Physical urticarias and cholinergic urticaria. *Immunol Allerg Clin North Am* 34(1):73–88
30. Nutong R, Mungthin M, Hatthachote P, Ukritchon S, Imjaijit W, Tengtrakulcharoen P, Panichkul S, Putwatana P, Prapaipanich W, Rangsin R (2018) Personal risk factors associated with heat-related illness among new conscripts undergoing basic training in Thailand. *PLoS ONE* 13(9):1–15
31. Leon LR, Bouchama A (2015) Heat stroke. *Compr Physiol* 5(2):611–647
32. Bach V, Libert JP (2022) Hyperthermia and heat stress as risk factors for sudden infant death syndrome: a narrative review. *Front Pediatr* 10:1–15
33. Maughan RJ (2003) Impact of mild dehydration on wellness and on exercise performance. *Eur J Clin Nutr* 57:19–23
34. Sandercock DA, Hunter RR, Nute GR, Mitchell MA, Hocking PM (2001) Acute heat stress-induced alterations in blood acid-base status and skeletal muscle membrane integrity in broiler chickens at two ages: implications for meat quality. *Poult Sci* 80(4):418–425
35. Hussain I, Ma X, Luo Y, Luo Z (2020) Fabrication and characterization of glycogen-based elastic, self-healable, and conductive hydrogels as a wearable strain-sensor for flexible e-skin. *Polymer* 210:122961
36. Liu Y, Wong TH, Huang X, Yiu CK, Gao Y, Zhao L, Zhou J, Park W, Zhao Z, Yao K, Li H, Jia H, Li J, Li J, Huang Y, Wu M, Zhang B, Li D, Zhang C, Yu X (2022) Skin-integrated, stretchable, transparent triboelectric nanogenerators based on ion-conducting hydrogel for energy harvesting and tactile sensing. *Nano Energy* 99:107442
37. Bai Z, Wang X, Zheng M, Yue O, Huang M, Zou X, Cui B, Xie L, Dong S, Shang J, Gong G, Blocki AM, Guo J, Liu X (2023) Mechanically robust and transparent organohydrogel-based E-Skin nanoengineered from natural silk. *Adv Funct Mater* 33(15):2212856
38. Lee GH, Woo H, Yoon C, Yang C, Bae JY, Kim W, Lee DH, Kang H, Han S, Kang SK, Park S, Kim HR, Jeong JW, Park S (2022) A personalized electronic tattoo for healthcare realized by on-the-spot assembly of an intrinsically conductive and durable liquid-metal composite. *Adv Mater* 34(32):1–10
39. Xu X, Yang T, Yu Y, Xu W, Ding Y, Hou H (2017) Aqueous solution blending route for preparing low dielectric constant films of polyimide hybridized with polytetrafluoroethylene. *J Mater Sci-Mater Electron* 28(17):12683–12689
40. Lim S, Son D, Kim J, Lee YB, Song JK, Choi S, Lee DJ, Kim JH, Lee M, Hyeon T, Kim DH (2015) Transparent and stretchable interactive human machine interface based on patterned graphene heterostructures. *Adv Funct Mater* 25(3):375–383
41. Schwartz G, Tee BCK, Mei J, Appleton AL, Kim DH, Wang H, Bao Z (2013) Flexible polymer transistors with high pressure sensitivity for application in electronic skin and health monitoring. *Nat Commun* 4(1859):1–8
42. Emrich HM, Stoll E, Friolet B, Colombo JP, Richterigh R, Rossi E (1968) Cystic fibrosis of the salt metabolism pancreas sweat gland membrane transport sweat rate sweat composition in relation to rate of sweating in patients with cystic fibrosis of the pancreas. *Pediatr Res* 2:464–478

Publisher's Note

Springer Nature remains neutral with regard to jurisdictional claims in published maps and institutional affiliations.

Submit your manuscript to a SpringerOpen® journal and benefit from:

- Convenient online submission
- Rigorous peer review
- Open access: articles freely available online
- High visibility within the field
- Retaining the copyright to your article

Submit your next manuscript at ► [springeropen.com](https://www.springeropen.com)